# On the Corner Elements of the CKM and PMNS Matrices*

Michael J BAKER† and José BORDES‡
*Departament Fisica Teorica and IFIC, Centro Mixto CSIC, Universitat de Valencia, Calle Dr. Moliner 50, E-46100 Burjassot (Valencia), Spain*

CHAN Hong-Mo§
*Rutherford Appleton Laboratory, Chilton, Didcot, Oxon, OX11 0QX, United Kingdom*

TSOU Sheung Tsun¶
*Mathematical Institute, University of Oxford, 24-29 St. Giles', Oxford, OX1 3LB, United Kingdom*

(Dated: June 4, 2012)

Recent experiments show that the top-right corner element ($U_{e3}$) of the PMNS, like that ($V_{ub}$) of the CKM, matrix is small but nonzero, and suggest further via unitarity that it is smaller than the bottom-left corner element ($U_{\tau 1}$), again as in the CKM case ($V_{ub} < V_{td}$). An attempt in explaining these facts would seem an excellent test for any model of the mixing phenomenon. Here, it is shown that if to the assumption of a universal rank-one mass matrix, long favoured by phenomenologists, one adds that this matrix rotates with scale, then it follows that (A) by inputting the mass ratios $m_c/m_t, m_s/m_b, m_\mu/m_\tau$, and $m_2/m_3$, (i) the corner elements are small but nonzero, (ii) $V_{ub} < V_{td}$, $U_{e3} < U_{\tau 1}$, (iii) estimates result for the ratios $V_{ub}/V_{td}$ and $U_{e3}/U_{\tau 1}$, and (B) by inputting further the experimental values of $V_{us}, V_{tb}$ and $U_{e2}, U_{\mu 3}$, (iv) estimates result for the values of the corner elements themselves. All the inequalities and estimates obtained are consistent with present data to within expectation for the approximations made.



The purpose of this note is to try to understand the smallness of the corner elements of the quark [1, 2] and lepton [3, 4] mixing matrices and their asymmetry about the diagonals. It is shown that a scheme with a rank-one rotating mass matrix (R2M2) devised to explain the hierarchical masses and mixing of fermions [5] will automatically also give, as a bonus, the said asymmetry correctly.

To theoreticians, the mixing matrices of quarks and leptons are a bit of an embarrassment. While their experimental colleagues have improved the measurements of the CKM matrix elements to an impressive accuracy and gained an increasingly clear picture even of the PMNS matrix, which is incredibly difficult to acquire, no commonly accepted theoretical understanding has been achieved even of the qualitative features, let alone a calculation of the matrix elements to the accuracy now measured in experiment.

The latest injection from experiment is a batch of impressive new results, in order of appearance [6–10], which give a nonzero value for the upper corner element usually called $U_{e3}$ of the PMNS matrix. Now this $U_{e3}$ was widely expected to vanish based on some symmetry arguments which treated the mixing of leptons differently from that of quarks [11]. The new measured value for this, however, is in fact much larger in magnitude than the corresponding element $V_{ub}$ in the CKM matrix. Indeed, a combined fit by Blondel [12] of the first 4 experiments gives a value of:

$$\sin^2(2\theta_{13}) = 0.084 \pm 0.014. \tag{1}$$

If we take this central value of $\theta_{13}$ and assume, as some of these experiments do, that $\sin^2(2\theta_{23}) = 1$ and the CP phase $\delta = 0$, we get the PMNS matrix as:

$$U_{\rm PMNS} = \begin{pmatrix} 0.820 & 0.554 & 0.146 \\ 0.482 & 0.528 & 0.699 \\ 0.310 & 0.644 & 0.699 \end{pmatrix}, \tag{2}$$

as compared to the measured CKM matrix given in [13]:

$$V_{\rm CKM} = \begin{pmatrix} 0.97428 & 0.2253 & 0.00347 \\ 0.2252 & 0.97345 & 0.0410 \\ 0.00862 & 0.0403 & 0.999152 \end{pmatrix}, \tag{3}$$

where in all cases the central values of the matrix elements are given. For these we quote only their absolute values, as we shall deal mainly with these, only returning to the important question of the Kobayashi–Maskawa CP-violating phase [4] at the end.

One notes that the two matrices (2) and (3) share some qualitative features. In both, the corner elements are rather small, and have the same sign of asymmetry about the diagonal. (It is enough to look at the corner elements since the asymmetry in the other elements would then follow by unitarity, the norms of all rows and columns

* Work supported in part by Spanish MICINN and FEDER (EC) under grant FPA2011-23596 and Generalitat Valenciana under grant GVPROMETEO2010-056.

† michael.baker@uv.es
‡ jose.m.bordes@uv.es
§ h.m.chan@stfc.ac.uk
¶ tsou@maths.ox.ac.uk

being unity). In both matrices, the bottom-left corner element is larger than the top-right corner element by about a factor of 2. This asymmetry, together with the small values of the corner elements, are what particularly interest us here, for the prediction of both would be a delicate test no *ad hoc* model is likely to reproduce.

The similarity between the two matrices suggests, to us at least, that they be treated similarly and understood together as two facets of the same phenomenon, and the R2M2 scheme is an attempt to do so. We will give first a very brief outline of this scheme to facilitate future discussions. For details, the reader is referred to [5], a recent review.

The R2M2 scheme was suggested some years [14–16] ago as a possible explanation for the hierarchical mass spectrum and mixing pattern of quarks and leptons observed in experiment and incorporated *per se* into the standard model. We note first that any fermion mass matrix can, by a judicious relabelling of the $su(2)$ singlet right-handed fields, be cast into a form with no dependence on $\gamma_5$ [17] so that any rank-one mass matrix can be written without loss of generality in the form

$$m = m_T \boldsymbol{\alpha}\boldsymbol{\alpha}^\dagger, \tag{4}$$

in terms of a unit vector $\boldsymbol{\alpha}$ in generation space. This means that there is only one massive generation. With $\boldsymbol{\alpha}$ "universal" in the sense of being independent of the fermion types $T$ (i.e., whether up or down, or whether leptons or quarks), it further implies that there is no mixing between up and down states. Now such a form of the fermion mass matrix has long been suggested by phenomenologists [18, 19] as a good starting point for understanding mass hierarchy and mixing. What R2M2 adds to this is that the vector $\boldsymbol{\alpha}$ rotates with changing scales under renormalization.

How R2M2 can lead to mixing and mass hierarchy can be seen most simply by considering just the two heaviest generations, and assuming for further simplification that $\boldsymbol{\alpha}$ is real and that $m_T$ is scale-independent. The eigenvector $\boldsymbol{\alpha}$ at scale $\mu = m_t$ is the state vector $\mathbf{t}$ of $t$, and the orthogonal vector $\mathbf{c}$ is that of $c$. As the scale decreases, $\boldsymbol{\alpha}$ rotates through an angle, say $\theta_{tb}$, when it reaches the scale $\mu = m_b$, where it becomes the state vector $\mathbf{b}$ of $b$. The vector orthogonal to $\mathbf{b}$ is then the state vector $\mathbf{s}$ of $s$. We have therefore two dyads, $\{\mathbf{t}, \mathbf{c}\}$ and $\{\mathbf{b}, \mathbf{s}\}$, linked by the non-identity mixing matrix

$$\begin{pmatrix} V_{cs} & V_{cb} \\ V_{ts} & V_{tb} \end{pmatrix} = \begin{pmatrix} \mathbf{c}\cdot\mathbf{s} & \mathbf{c}\cdot\mathbf{b} \\ \mathbf{t}\cdot\mathbf{s} & \mathbf{t}\cdot\mathbf{b} \end{pmatrix} = \begin{pmatrix} \cos\theta_{tb} & -\sin\theta_{tb} \\ \sin\theta_{tb} & \cos\theta_{tb} \end{pmatrix}, \tag{5}$$

which is the 2-generation analogue of the CKM matrix.

As to hierarchical masses, denoting by $m_U$ and $m_D$ the values of $m_T$ for $U$ and $D$ type quarks, we have $m_t = m_U$ and $m_b = m_D$. At $\mu = m_t$ the eigenvector $\mathbf{c}$ has zero eigenvalue, but this is not the mass of the $c$ state, which should be evaluated at $\mu = m_c$. Indeed, $m_c$ is to be taken as the solution to the equation

$$\mu = \langle \mathbf{c}|m(\mu)|\mathbf{c}\rangle = m_U |\langle \mathbf{c}|\boldsymbol{\alpha}(\mu)\rangle|^2. \tag{6}$$

A nonzero solution exists since the scale on the LHS decreases from $\mu = m_t$ while the RHS increases from zero at that scale. At $\mu < m_t$ the vector will have rotated from $\mathbf{t}$ to a different direction so that it will have acquired a nonzero component, say $\sin\theta_{tc}$, in the direction of $\mathbf{c}$ giving

$$m_c = m_t \sin^2\theta_{tc}. \tag{7}$$

Further $m_c$ will be small if the rotation is not too fast. Similarly for $m_s$.

An interesting point to note here is that the mass matrix (4) remains rank-one throughout. Yet, simply because the mass matrix rotates, the lower generation $c$ acquires a nonzero mass, as if by "leakage" from the heavy state $t$. This "leakage mechanism" is a very special property of R2M2 to which we shall have occasion to return.

Basically the same arguments apply to the realistic case when all 3 generations are taken into account, although the analysis becomes a little more complicated. As the scale changes, the unit vector $\boldsymbol{\alpha}$ now traces out a curve on the unit sphere, which can bend in two directions, either along the sphere or sideways, and it can also twist, and it is these contortions of the rotation trajectory as the scale changes which will now determine the fermion mass and mixing patterns. Nevertheless, applying exactly the same physical arguments as before, one deduces, say for the $U$-type quarks, the following formulae

$$\begin{aligned} \mathbf{t} &= \boldsymbol{\alpha}(m_t), \\ \mathbf{c} &= \mathbf{u}\times\mathbf{t}, \\ \mathbf{u} &= \frac{\boldsymbol{\alpha}(m_c)\times\boldsymbol{\alpha}(m_t)}{|\boldsymbol{\alpha}(m_c)\times\boldsymbol{\alpha}(m_t)|}, \end{aligned} \tag{8}$$

and

$$\begin{aligned} m_t &= m_U, \\ m_c &= m_U |\boldsymbol{\alpha}(m_c)\cdot\mathbf{c}|^2, \\ m_u &= m_U |\boldsymbol{\alpha}(m_u)\cdot\mathbf{u}|^2. \end{aligned} \tag{9}$$

Together, these 2 sets of coupled equations allow us to evaluate both the state vectors and the masses. Similar equations and remarks apply also to $D$-type quarks as well as to the leptons. With the state vectors so determined, the mixing matrices can then be evaluated, e.g., for quarks:

$$V_{\rm CKM} \sim \begin{pmatrix} \mathbf{u}\cdot\mathbf{d} & \mathbf{u}\cdot\mathbf{s} & \mathbf{u}\cdot\mathbf{b} \\ \mathbf{c}\cdot\mathbf{d} & \mathbf{c}\cdot\mathbf{s} & \mathbf{c}\cdot\mathbf{b} \\ \mathbf{t}\cdot\mathbf{d} & \mathbf{t}\cdot\mathbf{s} & \mathbf{t}\cdot\mathbf{b} \end{pmatrix}. \tag{10}$$

The expression for the lepton mixing matrix $U_{\rm PMNS}$ would be similar.

An unusual outcome of the R2M2 hypothesis, as outlined above, is in giving nonzero masses to all fermions while the fermion mass matrix itself remains of rank one and chiral invariant throughtout. At first sight, this may seem counter-intuitive, due to the unfamiliarity of the

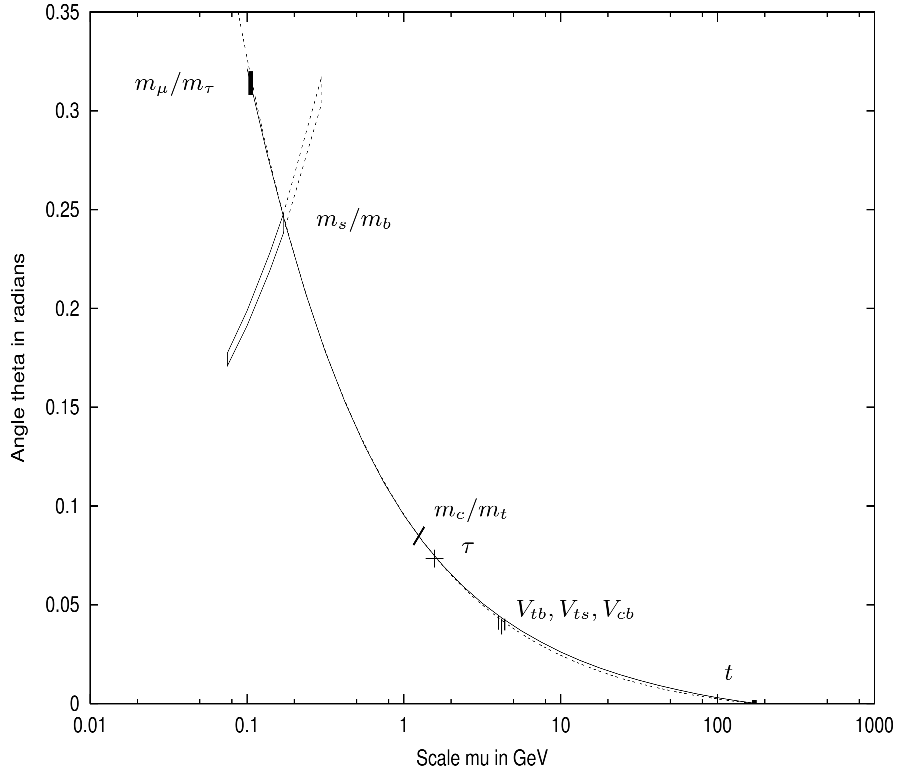


FIG. 1. The planar rotation curve taken from [20] for illustration. The solid curve shown was the best (exponential) fit to the data, which have not changed much since then, except for the point $m_s/m_b$ which figures little in the fit because of its large errors. The dotted curve was a fit with a phenomenological (but theoretically incomplete) model then being worked on, which is by now largely superseded.

new conditions introduced by a rotating mass matrix, which require a revision of some common notions deduced earlier from mass matrices which do not rotate. For a discussion of these points which, though straightforward, need some patience to go through, the reader is referred elsewhere, e.g. to [5], especially section 1.4 therein.

That the mass spectra and mixing matrices so obtained from a rank-one rotating mass matrix (R2M2) actually do resemble those observed in experiment can be checked in two ways: (i) invent a model trajectory, then evaluate in the manner indicated the mass spectra and mixing matrices of quarks and leptons to compare with experiment, or conversely, (ii) fit a trajectory through the experimental data on these quantities. Both have been tried with encouraging success [5, 16, 21]. We quote here in Figure 1 a particularly simple example from an early work [20] which will be of use to us later. As seen in this figure, the rotation angle $\theta$ obtained via (5) and (7) from the experimental masses and mixing angles in the 2-generation simplification all fall on a smooth curve as a function of $\mu$ as expected.

However, both the above methods (i) and (ii) for testing the R2M2 hypothesis involve some manipulations of the data or assumptions about the shape of the rotation trajectory, and may in the process obscure somewhat the basic simplicity of the result. What we wish to do here, in contrast, is to so drastically simplify the argument as to make the correlations between the various bits of data immediately obvious, in particular those in relation to the corner elements of the mixing matrices. To do so, we rely on the fact that most of the rotation angles involved are relatively small so that use can be made [22] of the differential Serret–Frenet–Darboux formulae for curves lying on a surface [23].

At every point of the trajectory for $\boldsymbol{\alpha}$, we set up a Darboux triad, consisting of first the normal to the surface $\mathbf{n}$, then the tangent vector $\boldsymbol{\tau}$ to the trajectory, and thirdly the normal $\boldsymbol{\nu}$ to both the above, normalized and orthogonal to one another. The Serret–Frenet–Darboux formulae then say

$$\begin{aligned} \mathbf{n}' &= \mathbf{n}(s+\delta s) = \mathbf{n}(s) - \kappa_n \boldsymbol{\tau}(s)\,\delta s + \tau_g \boldsymbol{\nu}(s)\,\delta s, \\ \boldsymbol{\tau}' &= \boldsymbol{\tau}(s+\delta s) = \boldsymbol{\tau}(s) + \kappa_n \mathbf{n}(s)\,\delta s + \kappa_g \boldsymbol{\nu}(s)\,\delta s, \\ \boldsymbol{\nu}' &= \boldsymbol{\nu}(s+\delta s) = \boldsymbol{\nu}(s) - \kappa_g \boldsymbol{\tau}(s)\,\delta s - \tau_g \mathbf{n}(s)\,\delta s, \end{aligned} \quad (11)$$

to first order in $\delta s$, a small increment in the arc-length $s$, where $\kappa_n$ is known as the normal curvature (bending along the surface), $\kappa_g$ the geodesic curvature (bending sideways) and $\tau_g$ the geodesic torsion (twist). For the special case here of a curve on the unit sphere, the surface normal $\mathbf{n}$ is the radial vector $\boldsymbol{\alpha}$, $\kappa_n = 1$ and $\tau_g = 0$, so that the formulae reduce to

$$\begin{aligned}\boldsymbol{\alpha}' &= \boldsymbol{\alpha}(s+\delta s) = \boldsymbol{\alpha}(s) - \boldsymbol{\tau}(s)\,\delta s,\\ \boldsymbol{\tau}' &= \boldsymbol{\tau}(s+\delta s) = \boldsymbol{\tau}(s) + \boldsymbol{\alpha}(s)\,\delta s + \kappa_g \boldsymbol{\nu}(s)\,\delta s,\\ \boldsymbol{\nu}' &= \boldsymbol{\nu}(s+\delta s) = \boldsymbol{\nu}(s) - \kappa_g \boldsymbol{\tau}(s)\,\delta s.\end{aligned} \tag{12}$$

At $\mu = m_t$, we recall that $\boldsymbol{\alpha}$ coincides with the state vector $\mathbf{t}$ for the $t$ quark. As the three quarks $t$, $c$ and $u$ are by definition independent quantum states, the state vectors $\mathbf{c}$ and $\mathbf{u}$ must be orthogonal to $\boldsymbol{\alpha}$ and to each other. They must therefore be related to $\boldsymbol{\tau}$ and $\boldsymbol{\nu}$ by a rotation about $\boldsymbol{\alpha}$ by an angle, say $\omega_U$,

$$(\mathbf{t},\mathbf{c},\mathbf{u}) = (\boldsymbol{\alpha}, \cos\omega_U \boldsymbol{\tau} + \sin\omega_U \boldsymbol{\nu}, \cos\omega_U \boldsymbol{\nu} - \sin\omega_U \boldsymbol{\tau}). \tag{13}$$

Similarly, for the $D$-type quarks we can write

$$(\mathbf{b},\mathbf{s},\mathbf{d}) = (\boldsymbol{\alpha}', \cos\omega_D \boldsymbol{\tau}' + \sin\omega_D \boldsymbol{\nu}', \cos\omega_D \boldsymbol{\nu}' - \sin\omega_D \boldsymbol{\tau}'), \tag{14}$$

where $\{\boldsymbol{\alpha}', \boldsymbol{\tau}', \boldsymbol{\nu}'\}$ is the Darboux triad taken at $\mu = m_b$, and $\omega_D$ is the corresponding rotation angle about $\boldsymbol{\alpha}'$.

Now the angle $\theta_{tb}$ between $\mathbf{t}$ and $\mathbf{b}$, which on the unit sphere is also the arc-length between the two, is envisaged in the rotation scheme to be rather small. As seen in Figure 1, the rotation angle deduced from data seems to approach an asymptote at $\mu = \infty$, the best fit to the data there being in fact an exponential. The rotation will speed up as $\mu$ decreases, but for $\mu$ between $m_t$ and $m_b$, the rotation remains rather small. Indeed, according to (5) it is given by the CKM matrix element $V_{tb} = \cos\theta_{tb}$. Experimentally, as seen above in (3), this is measured to have the value

$$V_{tb} = 0.999152^{+0.000030}_{-0.000045}, \tag{15}$$

which gives

$$\theta_{tb} = \delta s \sim 0.04119^{+0.000166}_{-0.000075}. \tag{16}$$

To this order of smallness then, we can take the expressions in (12) as the Darboux triad at $\mu = m_b$ and hence (14) as the $D$-triad. This gives immediately the CKM matrix, according to (10), as

$$V_{\rm CKM} = \begin{pmatrix} \cos(\omega) - \kappa_g \sin(\omega)\,\theta_{tb} & \sin(\omega) + \kappa_g \cos(\omega)\,\theta_{tb} & \sin(\omega_U)\,\theta_{tb} \\ -\sin(\omega) - \kappa_g \cos(\omega)\,\theta_{tb} & \cos(\omega) - \kappa_g \sin(\omega)\,\theta_{tb} & -\cos(\omega_U)\,\theta_{tb} \\ -\sin(\omega_D)\,\theta_{tb} & \cos(\omega_D)\,\theta_{tb} & 1 \end{pmatrix} \tag{17}$$

with $\omega = \omega_D - \omega_U$.

Although correct only to first order in $\theta_{tb}$, (17) exhibits succinctly some of the special properties arising from rotation with clear correspondence with experiment, which we shall now examine. We shall do so step-by-step starting with the least inputs and assumptions to get the general patterns, and then proceeding to more inputs and assumptions to get actual estimates.

First, on the immediate level, simply by virtue of the fact that $\theta_{tb}$ is small, we note already that (i) the off-diagonal elements in the last row and the last column are all of order $\theta_{tb}$ and therefore small compared to the others, (ii) the three diagonal elements are markedly different, the first two being equal to first order in $\theta_{tb}$, and both differing from unity by an amount of the same order, while the last stands alone, differing from unity by only order $\theta_{tb}^2$, (iii) the elements $V_{us}$ and $V_{cd}$ are equal also to first order in $\theta_{tb}$. A glance at (3) shows that these are all in agreement with what is experimentally observed.

Next, focussing now on the corner elements:

$$\begin{aligned} V_{ub} &= \mathbf{u}\cdot\mathbf{b} = \sin(\omega_U)\,\theta_{tb},\\ V_{td} &= \mathbf{t}\cdot\mathbf{d} = -\sin(\omega_D)\,\theta_{tb},\end{aligned} \tag{18}$$

we recall that $\omega_U$ is the angle between the two vectors $\mathbf{c}$ and $\boldsymbol{\tau}$ on the plane orthogonal to $\boldsymbol{\alpha} = \mathbf{t}$, where $\boldsymbol{\tau}$ is the tangent to the trajectory at $\mu = m_t$ and $\mathbf{c}$, by (8) above, is the vector lying on the plane containing the vectors $\boldsymbol{\alpha}(\mu = m_t)$ and $\boldsymbol{\alpha}(\mu = m_c)$. In other words, the angle $\omega_U$ arises as a consequence of the rotation of the vector $\boldsymbol{\alpha}(\mu)$ as $\mu$ changes from $m_t$ to $m_c$, and is thus generically of the same order of magnitude as $\theta_{tc}$ which, according to (7) or (9) above, gives rise to the mass ratio $m_c/m_t$. The same conclusion applies to $\omega_D$, namely that it should be of the same order as $\theta_{bs}$ which gives rise to the mass ratio $m_s/m_b$. Hence it follows that the two corner elements must both be particularly small compared with the others, since they are respectively of order $\theta_{tb}\,\theta_{tc}$ and $\theta_{tb}\,\theta_{bs}$ where both the angles in each of the products are small as a result of the rotation scenario. These corner elements are small basically because they are given by the twist of the trajectory, and the geodesic torsion $\tau_g$ being zero on a sphere, the twist can only arise as a second order effect of the rotation. We have thereby a ready explanation in the rotation scheme for why the corner elements in the CKM matrix are so particularly small, as experimentally observed.

As a corollary of both $\omega_U$ and $\omega_D$ being small, it follows from (17) that the elements $V_{cb}$ and $V_{ts}$ will have about the same value as $\theta_{tb}$, i.e., by (16) $\sim 0.041$, again as experimentally observed in (3). That estimates can be made on these two elements so immediately, but not on the two similarly-placed elements $V_{us}, V_{cd}$, comes about in the rotation scenario because the first pair is proportional to the normal curvature $\kappa_n$ in the original Serret–Frenet–Darboux formulae (11), and $\kappa_n = 1$ on the unit sphere when applied to R2M2 in (12), while both elements of the second pair are proportional to the geodesic curvature $\kappa_g$ which can have any value, depending on the rotation trajectory, even on the unit sphere.

Going further, we notice in Figure 1 that rotation seems to be speeding up from $\mu \sim m_t$ to $\mu \sim m_b$. More concretely, taking the mass values in GeV,

$$\begin{aligned} m_t &= 172.9 \pm 0.6 \pm 0.9 \\ m_b &= 4.19^{+0.18}_{-0.06} \\ m_c &= 1.29^{+0.05}_{-0.11} \\ m_s &= 0.100^{+0.030}_{-0.020} \end{aligned} \quad (19)$$

cited by PDG [13], one obtains,

$$\begin{aligned} \theta_{tc} &\sim \sqrt{m_c/m_t} \;\sim\; 0.086^{+0.0019}_{-0.0039}, \\ \theta_{bs} &\sim \sqrt{m_s/m_b} \;\sim\; 0.154^{+0.023}_{-0.019}. \end{aligned} \quad (20)$$

Now in the rotation picture, as explained above, $\omega_U$ is closely related to $\theta_{tc}$ and $\omega_D$ to $\theta_{bs}$, so that in as much as $\theta_{tc} < \theta_{bs}$, so will

$$V_{ub} < V_{td}, \quad (21)$$

which is the correct asymmetry in the corner elements observed in experiment, again readily explained here by rotation.

As a corollary of (21), one can deduce from (17) that

$$V_{cb} > V_{ts}, \quad (22)$$

although this would also follow from unitarity, but the following inequalities

$$\frac{V_{ub}}{V_{td}} < \frac{V_{ts}}{V_{cb}} < \frac{V_{cd}}{V_{us}}, \quad (23)$$

implied as well by (21) and (17) are not so obvious, and are equally satisfied by experiment.

One can go further still to make a semi-quantitative estimate for the size of the asymmetry between the two corner elements as follows. The angles $\theta_{tc}$ and $\theta_{bs}$ are still fairly small, to which one can reasonably apply again the Serret–Ferret–Darboux formulae of (12). In particular, the second equation there for $\boldsymbol{\tau}(s+\delta s)$, giving the change in direction of the tangent vector $\boldsymbol{\tau}$ in terms of the rotation angle $\delta s$, resolves this change into two components, one along the radius of the sphere which is proportional to the normal curvature $\kappa_n$, the other "sideways" on the tangent plane orthogonal to $\boldsymbol{\alpha}$ which is proportional to the geodesic curvature $\kappa_g$, as illustrated in Figure 2(a).

What interests us here is the second component proportional to $\kappa_g$ which can be thought of as the change in direction of the tangent to the rotation curve, but now projected into the plane orthogonal to $\boldsymbol{\alpha}$, as depicted in Figure 2(b). The angle we are after is $\omega_U$, which is the angle between $\mathbf{c}$, the state vector of the $c$ quark, and the original tangent vector $\boldsymbol{\tau}$. This is easily seen in Figure 2(b), as can be checked also by an explicit calculation using elementary differential geometry, to have half the value of the change in direction of the tangent vector itself, in the limit when the latter value is small. Hence, we have the result

$$\omega_U = \tfrac{1}{2}\kappa_g \theta_{tc}. \quad (24)$$

Similarly, of course,

$$\omega_D = \tfrac{1}{2}\kappa_g \theta_{bs}, \quad (25)$$

although in this case $\kappa_g$ should in principle refer to the geodesic curvature taken at $\mu = m_b$, not at $\mu = m_t$ as in the equation above. However, if we ignore this difference, which is of order $\theta_{tb}$ compared with $\kappa_g$ and therefore negligible to the order we are working, we obtain

$$\frac{V_{ub}}{V_{td}} \sim \frac{\sin\omega_U}{\sin\omega_D} \sim \frac{\sin\theta_{tc}}{\sin\theta_{bs}}. \quad (26)$$

Taking the estimates obtained before in (20) for these angles one then obtains the following estimate compared to experiment,

$$\left[\frac{V_{ub}}{V_{td}}\right]_{\rm est} \sim 0.56 \pm 0.01; \quad \left[\frac{V_{ub}}{V_{td}}\right]_{\rm exp} = 0.40 \pm 0.03. \quad (27)$$

This is as close an agreement as one can expect, since the starting formulae (12) are correct only to order $\delta s \sim \theta_{tb}$ and from (16) one would expect an error in the matrix elements of the order of $\theta_{tb}^2 \sim 0.0017$, which is not much smaller than the actual values of the matrix elements themselves.

So far one has input from experiment only the values of the mass ratios (20) and the fact that $\theta_{tb}$ is small. One can go even further still to estimate the actual values of the corner elements by inputting in addition $\theta_{tb}$ from (16) to set the scale and, say, the Cabibbo angle $V_{us}$ from (3) to estimate the value of the geodesic curvature $\kappa_g$. Indeed, using the formulae for $V_{us}$ in (17), and for $\omega_U, \omega_D$ in (24) and (25), one easily obtains

$$\kappa_g \sim 3.0, \quad (28)$$

which when substituted back into (24) and (25) will give

$$\omega_U \sim 0.128 \pm 0.004, \quad \omega_D \sim 0.23 \pm 0.03. \quad (29)$$

This then gives the following estimates for the actual values of the corner elements compared with experiment,

$$\begin{aligned} V_{ub}^{\rm est} &\sim 0.0053 \pm 0.0002, \quad V_{ub}^{\rm exp} = 0.00347^{+0.00016}_{-0.00012}; \\ V_{td}^{\rm est} &\sim 0.0094^{+0.0014}_{-0.0011}, \quad V_{td}^{\rm exp} = 0.00862^{+0.00026}_{-0.00020}. \end{aligned} \quad (30)$$

Again the agreement is about as good as can be expected, given the intrinsic errors in the starting Serret–Frenet–Darboux formulae of first order.

Now that one has reproduced by the above means the corner elements, one can proceed to give values to all elements of the CKM matrix. First from the estimated values of $\omega_U, \omega_D$ and of $\kappa_g$, one can evaluate the elements $V_{cb}$ and $V_{ts}$ as $(\cos\omega_U)\theta_{tb}$ and $(\cos\omega_D)\theta_{tb}$ by (17). For

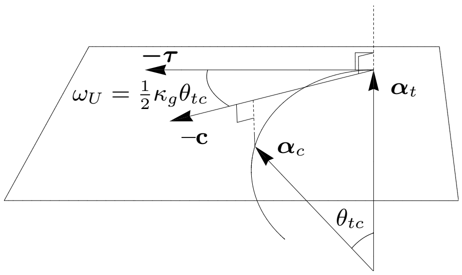


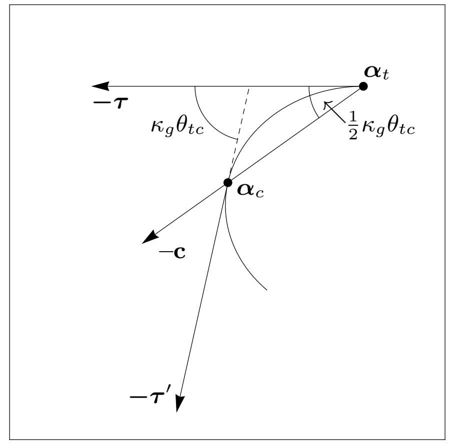


FIG. 2. Diagrams explaining the relation between $\kappa_g$ and the angle $\omega_U$: (a) how it looks in space; (b) projection of the relevant part into the tangent plane at $t$ orthogonal to $\boldsymbol{\alpha}(\mu = m_t)$. Here we write $\boldsymbol{\alpha}_t$ for $\boldsymbol{\alpha}(\mu = m_t)$ and $\boldsymbol{\alpha}_c$ for $\boldsymbol{\alpha}(\mu = m_c)$.

the other elements we shall make use of unitarity, i.e., the condition that that every row or column should have norm 1, rather than the formula (17) accurate only to order $\theta_{tb}$, because this will give the diagonal elements to a better accuracy. Indeed, even for the pair $V_{cb}$ and $V_{ts}$ we could have used unitarity applied to the last row and column in (17) because these satisfy unitarity already to order $\theta_{tb}^2$, and would have got identical results. Then applying unitarity to the remaining rows and columns, one obtains

$$V_{\rm CKM}^{\rm out} = \begin{pmatrix} 0.97427 & \mathit{0.2253} & 0.00530 \\ 0.2252 & 0.97346 & 0.0408 \\ 0.00943 & 0.0401 & \mathit{0.999152} \end{pmatrix}, \qquad (31)$$

where the entries in italics are inputs, the rest being evaluated as explained. This compares very well with (3) from experiment.

One sees thus, that with the simple formula (17) deduced from rotation, one can go already quite some way towards explaining the general features of the CKM matrix, in particular its corner elements and their asymmetry about its diagonal. In principle, the same arguments can be applied to the PMNS matrix for leptons as well, but there are a couple of serious reservations. First, the expansion parameter $\delta s$ is now given, in parallel to $\theta_{tb}$ above, by $U_{\tau 3}$ in (2) as $\sin\theta_{\tau 3} \sim 0.70$, which will take a lot of imagination to consider as a small expansion parameter. Secondly, on the physical masses of the neutrinos as given in experiment, the question arises whether they should be regarded as the Dirac masses which figure in the rotation formulae of (9) above, or as the masses obtained from these via some see-saw mechanism. This question matters in the estimate for the rotation angles $\theta_{\nu_3\nu_2}$ between $\nu_3$, the heaviest neutrino, and the next heaviest $\nu_2$, which is related to the Dirac masses. However, let us be cavalier here and boldly ignore the first reservation [1], while for the second, simply repeat the arguments for both the cases suggested.

Starting then from the experimental values of $m_\tau = 1.777$, $m_\mu = 0.106$ in GeV [12], we first obtain

$$\sin\theta_{\tau\mu} = \sqrt{m_\mu/m_\tau} = 0.244, \qquad (32)$$

the experimental errors here being negligible. Then taking the experimental neutrino mass differences [13],

$$\begin{aligned} \Delta m_{32}^2 &= (2.43 \pm 0.13) \times 10^{-3}\ \mathrm{eV}^2, \\ \Delta m_{21}^2 &= (7.59 \pm 0.21) \times 10^{-5}\ \mathrm{eV}^2, \end{aligned} \qquad (33)$$

and assuming normal hierarchy along with a negligible $m_1$ we obtain:

$$m_3 = 0.050 \pm 0.001\ \mathrm{eV}, \quad m_2 = 0.0087 \pm 0.0001\ \mathrm{eV}. \quad (34)$$

Hence for the Dirac case (D), we have straighforwardly:

$$\sin\theta_{\nu_3\nu_2}^{\rm D} = \sqrt{m_2/m_3} \sim 0.417 \pm 0.008. \qquad (35)$$

For the see-saw case (ss), we take for the see-saw mechanism [24] the simplest model, i.e., Type I quadratic see-saw, where 3 right-handed neutrinos are introduced and where their mass matrix is assumed to be proportional to the identity $3 \times 3$ matrix. This then gives the physical masses of the 3 neutrino states $\nu_i$ as respectively

[1] This cavalier attitude is not really necessary, except here for the sake of simplicity and transparency, for the Serret-Frenet-Darboux formulae can readily be integrated by numerical methods given some assumptions about the rotation trajectory. An investigation along these lines to reproduce the whole mixing matrix and the mass spectrum of both quarks and leptons is near completion, and a report is under preparation [25], but the results obtained on the corner elements are not qualitatively different from those given below.

$m_i = (m_i^{\rm D})^2/m_R$, with $m_i^{\rm D}$ being their Dirac masses and $m_R$ the right-handed neutrino mass. It follows therefore that their Dirac masses $m_i^{\rm D}$ are proportional to the square-root of their physical masses $m_i$ as given above in (34). And since it is the Dirac mass which enters in the rotation mechanism, we deduce that in the (ss) case:

$$\sin\theta^{\rm ss}_{\nu_3\nu_2} = \sqrt{m_2^{\rm D}/m_3^{\rm D}} = \sqrt{\sqrt{m_2/m_3}} = \sqrt{\sin\theta^{\rm D}_{\nu_3\nu_2}} \sim 0.646 \pm 0.006. \tag{36}$$

We note first that the error in this rotation angle induced by the experimental errors on neutrino masses is quite small, for both (D) and (ss), as to be entirely negligible for the purpose we shall make use of it to deduce the results below. Secondly, and more importantly, since for both cases (D and ss), $\sin\theta_{\tau\mu} < \sin\theta_{\nu_3\nu_2}$, it follows that the corner elements of the PMNS matrix will have the same asymmetry as in the CKM matrix, i.e. $U_{e3} < U_{\tau 1}$, as seems to be implied by experiment in (2). In fact, for the values adopted there for $\theta_{12}$ and $\theta_{23}$, this asymmetry will persist up to $\sin^2 2\theta_{13} = 0.23$ or to $\theta_{13} = 0.25$, i.e., way outside the experimental errors.

Secondly, accepting the result (25) obtained above even for this case, namely that the angles (36) can still be considered as small enough for the arguments in Figure 2 to apply, so that for charged leptons and neutrinos respectively we have:

$$\omega_U = \tfrac{1}{2}\kappa_g\theta_{\tau\mu}, \quad \omega_D = \tfrac{1}{2}\kappa_g\theta_{\nu_3\nu_2}, \tag{37}$$

and assuming again that $\kappa_g$ is the same for $U$ and $D$, we obtain

$$\frac{U_{e3}}{U_{\tau 1}} \sim \frac{\theta_{\tau\mu}}{\theta_{\nu_3\nu_2}} \sim 0.6 \text{ (D)}, \ 0.4 \text{ (ss)}, \tag{38}$$

as compared with the value 0.47 obtained for the matrix in (2) above and agreeing with the noted asymmetry. Lastly, pushing it all the way, if we repeat the previous arguments to estimate the values of the corner elements for the CKM matrix, inputting here in place of the Cabibbo angle the solar neutrino angle $\sin^2(2\theta_{12}) \sim 0.861$ [13], and in place of the element $V_{tb}$ the element $U_{\tau 3}$ as given in (2) obtained by unitarity from a maximal $U_{\mu 3}$ (the effect of the corner $U_{e3}$ being negligible in this calculation for the accuracy needed), we obtain the estimates

$$U_{e3}^{\rm D} \sim 0.06; \quad U_{e3}^{\rm ss} \sim 0.05. \tag{39}$$

These estimates, though obviously very crude, are not ridiculous, and maintain the above observation that the corner elements will be small and be asymmetric about the diagonal to roughly the order as seems indicated by experiment. Notice in particular that the corner elements here, just as in the CKM case before, have no reason to vanish as it has in some symmetry schemes, unless, of course, the geodesic curvature happens to be exactly zero at that point of the rotation trajectory under consideration while being nonzero both at $\mu = m_t$ and at $\mu = m_b$. Besides, if $\kappa_g = 0$, then according to (17) and (37), the solar neutrino angle $U_{e2}$ would vanish also, in gross contradiction to experiment.

In the above study of both the CKM and PMNS matrices, we notice that in arriving at the conclusion that the corner elements are small and have the right asymmetry, and differ from one another even by about the right ratios, one has input from experiment only $m_c/m_t, m_s/m_b$ for CKM, and $m_\mu/m_\tau, m_2/m_3$ for PMNS, mass ratios which have *a priori* nothing to do with the up-down mixing contained in the CKM and PMNS matrices, except via the R2M2 hypothesis. Hence, that one has come to the right conclusions can justly be regarded as a non-trivial test of the rotation hypothesis. To a lesser extent, perhaps, even the rough estimates for the sizes of the corner elements can also be regarded as such, for here one has input in addition from experiment only two other mixing matrix elements in each case, namely $V_{tb}, V_{us}$ for CKM and $U_{\tau 3}, U_{e2}$ for PMNS, which are not enough to determine via unitarity the corner elements.

Finally, we come to the important question of the CP-violating phase, which so far has been ignored. A very interesting point of the R2M2 hypothesis is that it also automatically provides an explanation for this phase, and in quite an intriguing manner, by relating it to the theta-angle of topological origin in the QCD action, thereby even offering a solution to the old strong CP problem. This comes about because R2M2 has the very distinctive property that the fermion mass matrix remains of rank one throughout, hence having two zero eigenvalues at every scale. These zero eigenstates, as is well-known [26], would allow the strong theta-angle to be eliminated by a chiral transformation without making the mass matrix complex. Yet, because of the "leakage mechanism" due to rotation described above in (7), none of the quarks need have a zero physical mass. Since the mass matrix rotates with scale, however, the chiral transformation, which is to be performed at every scale in the direction of the normal vector $\boldsymbol{\nu}$ of the Darboux triad at that scale, has to be scale-dependent. Hence, its effects will get transmitted on to the state vectors of the various quarks by rotation, and further on to the CKM matrix also, where they will appear as a CP-violating phase. The details of how this actually happens are explained in [5, 27] to which the reader is referred. However, whether a similar procedure applies also to leptons is at present unclear.

The beauty of the approximate formula (17) is that it allows the above effect of the chiral transformation required for eliminating the theta-term to be given explicitly. We first expand the $U$- and $D$-triads respectively in terms of the Darboux triads at $\mu = m_t$ and $\mu = m_b$. Then we apply to each the appropriate chiral transformation, each in the direction of the vector $\boldsymbol{\nu}$ at its own scale, giving for the relevant left-handed fields just a phase $\exp(-i\theta/2)$ to that component in the $\boldsymbol{\nu}$ direction,

$$
\begin{aligned}
(\mathbf{t}, \mathbf{c}, \mathbf{u}) &= (\boldsymbol{\alpha}, \cos\omega_U \boldsymbol{\tau} + \sin\omega_U \boldsymbol{\nu}\, e^{-i\theta/2}, \cos\omega_U \boldsymbol{\nu}\, e^{-i\theta/2} - \sin\omega_U \boldsymbol{\tau}), \\
(\mathbf{b}, \mathbf{s}, \mathbf{d}) &= (\boldsymbol{\alpha}', \cos\omega_D \boldsymbol{\tau}' + \sin\omega_D \boldsymbol{\nu}'\, e^{-i\theta/2}, \cos\omega_D \boldsymbol{\nu}'\, e^{-i\theta/2} - \sin\omega_D \boldsymbol{\tau}'). \qquad (40)
\end{aligned}
$$

The CKM matrix can then be evaluated with these two triads of state vectors as before by (10), but this will now contain a CP-violating phase.

To see what effect this phase so obtained will have, it would be easiest to evaluate the Jarlskog invariant corresponding to this matrix. Notice however that in the case of R2M2, where the orientation of the mass matrix is scale dependent, one cannot relate CP non-conservation directly to the commutator of the (hermitian) mass matrices, as it was originally proposed by C. Jarlskog in [28]. Instead, one has to rely solely on the unitary properties of the mixing matrix and work with the quartic rephasing invariants which are scale independent. These invariants appeared in earlier works on CP non-conservation [29] without mentioning the mass matrix commutator properties.

Suppose we take in particular the minor of the matrix at the bottom right, the elements of which are then given by (40) to be

$$V_{cb} = -\cos\omega_U\, \theta_{tb} \qquad (41)$$
$$V_{ts} = \cos\omega_D\, \theta_{tb} \qquad (42)$$
$$V_{tb} = 1 \qquad (43)$$
$$
\begin{aligned}
V_{cs} &= \cos(\omega_D - \omega_U) - \sin(\omega_D - \omega_U)\kappa_g\, \theta_{tb}\, \cos(\theta/2) \\
&\quad + i\sin(\omega_D + \omega_U)\kappa_g\, \theta_{tb}\, \sin(\theta/2). \qquad (44)
\end{aligned}
$$

We then arrive at the following explicit formula for the Jarlskog invariant [28]

$$
\begin{aligned}
J &= \mathrm{Im}\{V_{cs}\, V_{tb}\, V_{cb}^*\, V_{ts}^*\} \qquad (45) \\
&= -\cos\omega_U \cos\omega_D \sin(\omega_D + \omega_U)\, \kappa_g\, \theta_{tb}^3\, \sin(\theta/2). \qquad (46)
\end{aligned}
$$

Though approximate, this is much more compact and amenable than that obtained before in [5, 27]. For example, putting in the values given above for $\omega_U, \omega_D, \theta_{tb}$ and $\kappa_g$, one easily obtains

$$|J\,| \sim 7.1 \times \sin(\theta/2) \times 10^{-5}, \qquad (47)$$

which, for the strong CP angle $\theta$ of order unity, is of the order of the experimental value of $J \sim 2.9 \times 10^{-5}$ as given in [13]. Alternatively, inputting the experimental value, one arrives at the estimate of $|\theta| \sim 0.8$, which is indeed of order unity.

In principle one can redo the whole analysis above taking account of the CP-violating phase all through. Indeed we have done just that. However, rather than including the theta-term right at the beginning, we think it much more transparent to present our results in the way we did, knowing full well that for the accuracy we aim for at present, the effect of the CP phase will be small because of the smallness of $J$, and the absolute values of the CKM matrix elements displayed will not be much affected. This is confirmed by our calculations.

In summary, we conclude that the R2M2 (rotation) hypothesis gives automatically small but nonzero corner elements to both the CKM and PMNS matrices with the right asymmetry and roughly the right magnitudes as observed in experiment. This is, we believe, a nontrivial test for the hypothesis. The merit of the small angle approximation used here is the utter simplicity and transparency of its derivations, with the minimum of assumptions on the rotation trajectory and without resorting to numerical methods. Thus, though not giving as extensive and as accurate results, it is a valuable complement to the approach by numerical integration of the Serret-Frenet-Darboux formulae based on an explicit parametrization of the rotation trajectory [25].


[1] N. Cabibbo, Phys. Rev. Lett. **10**, 531 (1963).

[2] M. Kobayashi and K. Maskawa, Prog. Theor. Phys. **49**, 282 (1972).

[3] B. Pontecorvo, Zh. Eksp. Teor. Fiz. **33**, 549 (1957) and **34**, 247 (1958).

[4] Z. Maki, M. Nakagawa and S. Sakata, Progr. Theor. Phys. **28**, 870 (1962).

[5] Michael J Baker, José Bordes, Chan Hong-Mo and Tsou Sheung Tsun, Int. J. Mod. Phys. **A26**, 2087-2124 (2011), arXiv:1103.5615.

[6] K. Abe et al. (T2K Collaboration), Phys. Rev. Lett. **107**, 041801 (2011), arXiv:1106.2822 [hep-ex].

[7] P. Adamson et al. (MINOS Collaboration), Submitted to Phys. Rev. Lett., arXiv:1108.0015 [hep-ex].

[8] Y Abe et al. (Double Chooz Collaboration), arXiv:1112.6353 [hep-ex].

[9] FP An et al. (Daya-Bay Collaboration), Phys.Rev.Lett. 108, 171803 (2012); arXiv:1203.1669 [hep-ex].

[10] JK Ahn et al. (RENO Collaboration), arXiv:1204.0626 [hep-ex].

[11] P. F. Harrison, D. H. Perkins and W. G. Scott, Phys. Lett. **B530**, 167 (2002), hep-ph/0202074;
G. Altarelli and F. Feruglio, Rev. Mod. Phys. **82**, 2701-2729 (2010), arXiv:1002.0211 [hep-ph].

[12] In summary talk given by Alain Blondel at the Rencontres de Moriond EW2012, 3–10 March, 2012.

[13] K. Nakamura et al. (Particle Data Group), J. Phys. **G37**, 075021 (2010) and 2011 partial update for the 2012 edition; http://hepdata.cedar.ac.uk/lbl/

[14] Chan Hong-Mo and Tsou Sheung Tsun, Phys. Rev. D57, 2507, (1998), hep-th/9701120.

[15] José Bordes, Chan Hong-Mo, Jacqueline Faridani, Jakov Pfaudler, and Tsou Sheung Tsun, Phys. Rev. D58, 013004, (1998), hep-ph/9712276.

[16] J. Bordes, Chan Hong-Mo and Tsou Sheung Tsun, Eur. Phys. J. **C10**, 63 (1999), hep-ph/9901440.

[17] Steven Weinberg, Phys. Rev. **D7**, 2887 (1973).

[18] H. Fritsch, Nucl. Phys. **B155**, 189 (1978).

[19] H. Harari, H. Haut and J. Weyers, Phys. Lett. B **78**, 459 (1978).

[20] José Bordes, Chan Hong-Mo and Tsou Sheung Tsun, Eur. Phys. J. **C27**, 189-200 (2003), hep-ph/0203124.

[21] Michael J Baker and Tsou Sheung Tsun, Eur. Phys. J. **C70**, 1009–1015 (2010); DOI 10.1140/epjc/s10052-010-1506-0; arXiv:1005.2676v2 [hep-ph].

[22] José Bordes, Chan Hong-Mo, Jakov Pfaudler, and Tsou Sheung Tsun, Phys. Rev. D58, 053006, (1998), hep-ph/9802436.

[23] See, e.g., L.P. Eisenhart, *A Treatise on the Differential Geometry of Curves and Surfaces*, Ginn and Company 1909, Boston; M.P. do Carmo, *Differential Geometry of Curves and Surfaces*, Prentice-Hall 1976, Englewood Cliffs, New Jersey.

[24] M. Gell-Mann, P. Ramond and R. Slansky (1979), in Supergravity, edited by P. van Nieuwenhuizen and D.Z. Freedman, North Holland Publ. Co.; P. Minkowski, Phys. Lett. B 67 (1977) 421; R.N. Mohapatra and G. Senjanovic, Phy. Rev. Lett. 44 (1980) 912.

[25] Michael J Baker, José Bordes, Chan Hong-Mo and Tsou Sheung Tsun, in preparation.

[26] See, e.g., Steven Weinberg, *The Quantum Theory of Fields II* (Cambridge University Press, New York, 1996).

[27] José Bordes, Chan Hong-Mo and Tsou Sheung Tsun, Int. J. Mod. Phys. **A25** 5897-5911 (2010), arXiv:1002.3542 [hep-ph].

[28] C. Jarlskog, Z. Phys. **C29**, 491 (1985); Phys. Rev. Lett. **55**, 1039 (1985).

[29] *CP Violation*, ed. C. Jarlskog, World Scientific 1989, page 28 of Introduction by Jarlskog; C. Jarlskog, Z. Phys. **C29**, 491 (1985); Phys. Rev. Lett. **55**, 1039 (1985). See also E. P. Shabalin, Sov. J. Nucl. Phys. **28**, 75 (1978); R. H. Dalitz, Acta Physica Austriaca Suppl. XXIV, 393 (1982).